Curvature Condensation and Bifurcation in an Elastic Shell

Curvature Condensation and Bifurcation in an Elastic Shell

Moumita Das,[1] Ashkan Vaziri,[1] Arshad Kudrolli,[2] and L. Mahadevan[1,*]

[1]*Division of Engineering and Applied Sciences, Harvard University, Cambridge, Massachusetts 02138, USA*
[2]*Department of Physics, Clark University, Worcester, Massachusetts 01610, USA*

(Received 7 May 2006; published 5 January 2007)

We study the formation and evolution of localized geometrical defects in an indented cylindrical elastic shell using a combination of experiment and numerical simulation. We find that as a symmetric localized indentation on a semicylindrical shell increases, there is a transition from a global mode of deformation to a localized one which leads to the condensation of curvature along a symmetric parabolic defect. This process introduces a soft mode in the system, converting a load-bearing structure into a hinged, kinematic mechanism. Further indentation leads to twinning wherein the parabolic defect bifurcates into two defects that move apart on either side of the line of symmetry. A qualitative theory captures the main features of the phenomena but leads to further questions about the mechanism of defect nucleation.

DOI: 10.1103/PhysRevLett.98.014301 PACS numbers: 46.70.De, 46.32.+x, 46.70.Hg

The formation of defects in continuum physics has been the subject of long-standing investigation in many ordered and partially ordered bulk condensed matter systems such as crystals, liquid crystals, and various quantum ''super'' phases [1]. In low-dimensional systems, the formation and evolution of defects involves an extra level of complexity due to the interplay between geometry and physics and remains an active area of research. Even in simple physical systems such as the mundane paper on which we write and the textile sheets we wear daily, the visual effects of these defects are arresting; in Fig. 1 we see a heavy hanging drape with curved catenarylike wrinkles that themselves have creaselike anisotropic defects (see arrows) on scales much smaller than the crease but much larger than the thickness of the drape. This hierarchy in structural scales is common in many elastic systems and naturally suggests the question of how such structures form. While the shape, response, and stability of these structures has been the subject of much study recently [2–5], following the now classical work of Pogorelov [6], the process by which these defects arise from a featureless sheet is essentially unknown.

To address this question in the simple context of an everyday example, a thin mylar sheet is bent into a half-cylindrical elastic shell (thickness t, radius R, and length L, $t \ll R < L$; $R/t \sim 100$) that is clamped along its lateral edges. A pointlike probe that is free to slip on the mylar is then used to indent the sheet at one edge along the axis of symmetry as shown in Fig. 2(a)–2(d); preliminary investigations on a similar subject were conducted a while ago [7]. The shape of the sheet is then reconstructed using laser aided tomography [8], wherein a laser sheet is used to interrogate the surface and determine its height. A CCD camera with a resolution of 1024×768 pixels is used to image the reflected light and the laser sheet is rotated with a stepper motor which allows the entire surface to be scanned.

For small values of the indentation δ, the shell deforms strongly in the immediate neighborhood of the edge; away from the edge the curvature of the sheet decays monotonically [Fig. 2(a)]. As the indentation is increased beyond a critical threshold, a secondary maximum in the curvature appears along the axis of symmetry, but at a distance d_y away from the point of indentation [Fig. 2(b)]. This curvature ''condensate'' takes the form of a parabolic defect similar to that studied earlier in the context of crumpling [3,5]. For still larger values of the indentation, the parabolic defect bifurcates into two defects that move away symmetrically from the axis of the cylinder, in a manner analogous to defect twinning [Fig. 2(c)]. Finally, for even larger values of the indentation, the defects stop moving along the axis of the cylinder, and a large region of the shell folds inwards [Fig. 2(d)] about the now mature localized hinge that has formed at the defect. Since the long wavelength modes of deformation of a thin cylindrical shell associated with bending and stretching are both characterized by the Young's modulus E and thickness t [9], the only intrinsic dimensionless parameter is the ratio R/t; there is effectively no dependence on material parameters. This

FIG. 1 (color online). Condensation of curvature in a heavy drape. The smooth catenarylike folds with a single direction of localized curvature coexist with regions of curvature condensation, indicated by arrows, where curvature is strongly focused.

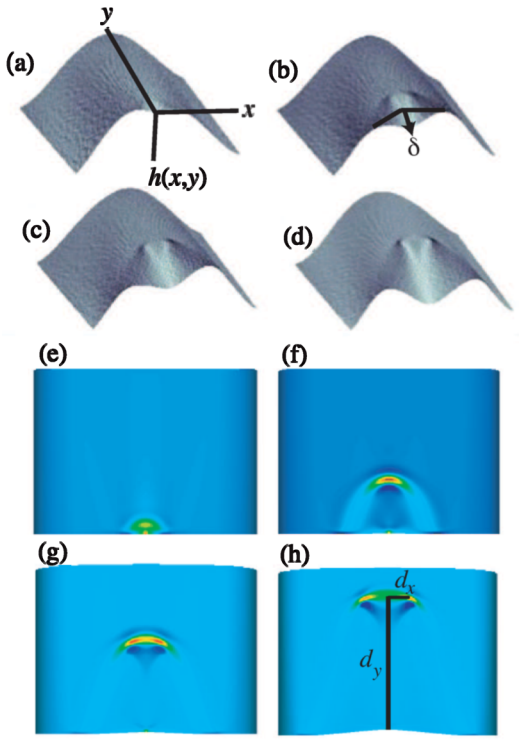

FIG. 2 (color online). Curvature condensation in an indented semicylinder. Figures (a)–(d) correspond to the experimentally determined deformation of the sheet with the colormap representing curvature $h_{,yy}$ along the axis of cylindrical symmetry. Figures (e)–(h) show the evolution of the curvature $h_{,yy}$ with increasing indentation δ (sheet viewed from the top), for $t/R = 0.001$ determined using numerical simulations (see text); red corresponds to high curvatures, blue to low. The Gauss curvature $\kappa_G \sim \frac{1}{R} h_{yy}$ shows the same qualitative trends in both cases.

makes the problem particularly attractive since geometry is at the heart of all the observed phenomena. However, the nonlinear equations for the deformations of shells [10] are analytically insoluble except in some special cases involving axisymmetric geometries and deformations. Therefore, we resort to a numerical investigation, and complement this with scaling analyses to tease out the qualitative aspects of our results. A commercially available finite element code ABAQUS is used to minimizes the elastic energy of the shell (made of a material that is assumed to be linearly elastic, with Young's modulus $E = 100$ MPa and Poisson's ratio $\nu = 0.3$) with an energy density

$$U = \frac{Et}{2(1-\nu^2)}[(\epsilon_1+\epsilon_2)^2 - 2(1-\nu)(\epsilon_1\epsilon_2 - \gamma^2)] + \frac{Et^3}{24(1-\nu^2)}[(\kappa_1+\kappa_2)^2 - 2(1-\nu)(\kappa_1\kappa_2 - \tau^2)].$$

Here the first line characterizes the energy associated with in-plane deformations (with strains ϵ_1, ϵ_2, γ) and the second line accounts for the energy associated with out-of-plane deformations (κ_1, κ_2, τ are the curvatures and twist relative to the undeformed tube). Four-node, quadrilateral shell elements with reduced integration and a large-deformation formulation were used in the calculations.

The results are shown in Fig. 2(e)–2(h): as the indentation is increased, the curvature condenses at a distance away from the edge, and this condensate bifurcates into two upon further indentation. To understand these transitions qualitatively, we note that a complete cylindrical shell that is pinched gently at one end responds by deforming globally in a nearly inextensional mode. Although a semicylinder clamped along its lateral edges also does the same when indented weakly, this global mode is screened by the lateral clamps. Strong indentation then leads to a transition from the global mode to a localized mode wherein the curvature localizes in a very small region at a distance d_y from the edge. In Fig. 3(a), we show that this transition arises only when the indentation is larger than a threshold.

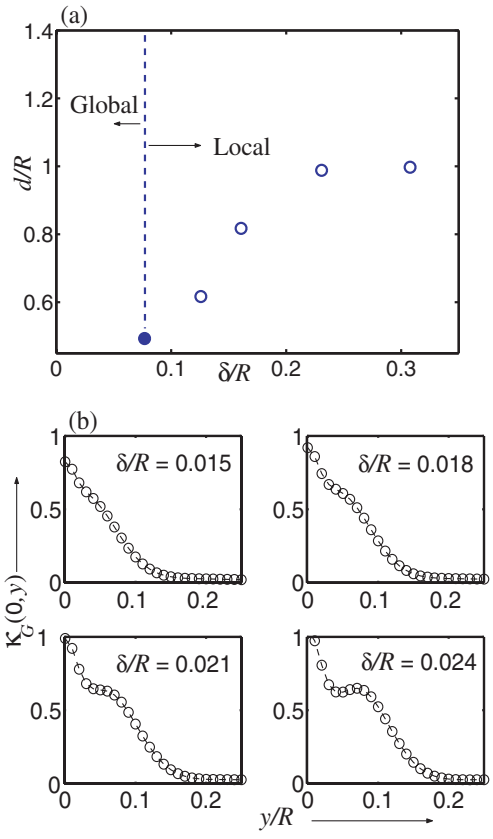

FIG. 3 (color online). Global and local modes of deformation. (a) Experimentally determined location of the condensate as a function of indentation depth, for a mylar sheet ($t/R \sim 0.01$). Filled symbols represent the condensate (before bifurcation) and open symbols represent the twinned state (after bifurcation). (b) We can understand this transition by probing the Gauss curvature along the axis of symmetry $\kappa_G(0, y) \sim \frac{1}{R} h_{,yy}(0, y)$ determined numerically. We see the transition from a global mode with just a single curvature maximum (at the point of indentation) to a localized mode of deformation with a secondary maximum in the curvature that arises when the indentation δ is larger than some threshold that is a function solely of the cylinder geometry. Here $t/R = 0.001$.

To further interrogate this phenomenon, in Fig. 3(b), we plot the Gauss curvature of the cylinder along the axis of symmetry $\kappa_G(0, y)$ as a function of the scaled indentation δ/R. For small indentations, we find that $\kappa_G(0, y)$ decreases monotonically away from the zone of indentation. However, as the indentation is increased, $\kappa_G(0, y)$ develops an inflection point and eventually a secondary maximum, where the curvature condensate forms. This condensation is not seen in one-dimensional elastic systems [11] where there is no analog of the Gauss curvature; it is crucially dependent on the two dimensionality of the problem. Associated with this condensation, an infinite-dimensional cylindrical structure with finite stiffness becomes a finite-dimensional mechanism, acquiring a new soft degree of freedom with a very low stiffness due to the formation of a hinge at the location of high curvature, which is akin to a condensed phase. There are thus rough analogies to a phase transition when interpreted in terms of the delocalized (gaseous) Gauss curvature and its localized (liquid) condensate.

As the cylindrical structure develops a hinge at location d_y in response to the indentation δ, geometry implies that $d_y \sim \delta$. Of course, as δ is increased further, we expect d_y to eventually saturate at a location $d_{y,\mathrm{sat}} \sim R$. In Fig. 4(a), we see that numerical simulations confirm these naïve expectations: for small indentations following the onset of localization, the location of the condensate increases linearly with δ before it eventually saturates with $d_{y,\mathrm{sat}} \sim R$. The location of the condensate is also a function of the cylinder thickness t; thicker, stiffer sheets lead to larger $d_{y,\mathrm{sat}}$. In Fig. 4(a), we see that $d_{y,\mathrm{sat}}$ is indeed larger for greater values of t since it is energetically favorable to have the curvature condense further from the indentation. For very thin sheets, the curvature condensate bifurcates into two condensates when the indentation $\delta > \delta_{\mathrm{bif}}$; each of the symmetric condensates moves away from the axis of symmetry, as can be seen in Fig. 4(b). The critical indentation δ_{bif} where the condensate bifurcates into two is found to follow the scaling $\delta_{\mathrm{bif}} \sim t^{1/2}$.

Zooming in on the region of curvature condensation, we observe that the curvature is localized along a parabolic crescent-shaped structure [Fig. 5(a)] similar to the core of a developable cone [3,5,12], where stress is focused anisotropically. Our simulations show that for a given indentation, the width of the parabolic defect $w \sim \sqrt{tR}$ [Fig. 5(b)], while its radius of curvature $R_p \sim 2t^{1/3}R^{2/3}$ [Fig. 5(c)], consistent with earlier results on the size of the core of the defect in a sheet bent into a cone [3,5,12]. In Fig. 5(d) we see that the scaled location of the curvature condensate $d/R \sim (t/R)^{-1/3}$.

We now seek a qualitative understanding of these results using the Donnell–Föppl–von Kármán equations that characterize the in- and out-of-plane deformations of a weakly curved sheet [13]. For the parabolic defect of high curvature, the elastic bending energy $E_B \approx Et^3(\frac{\delta}{dw})^2 dw$, where δ/dw is the dominant component of

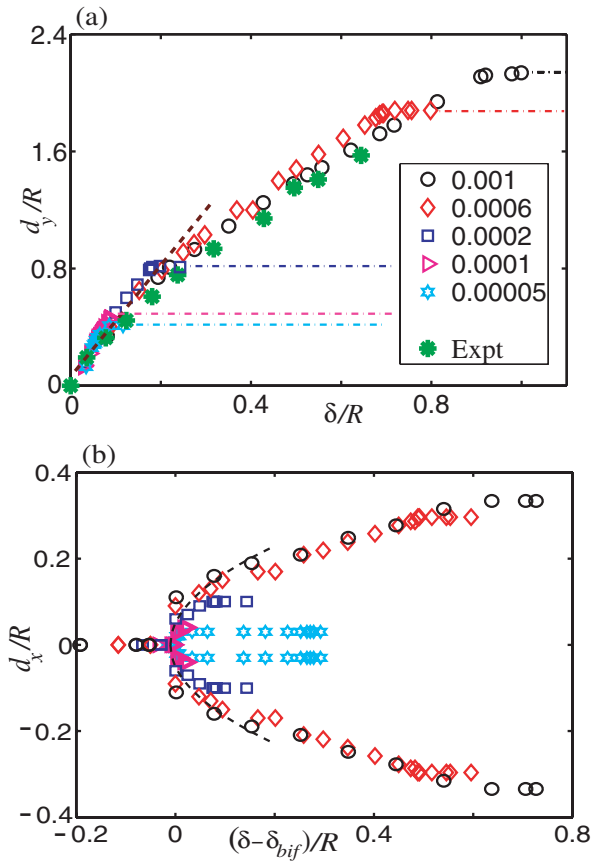

FIG. 4 (color online). Curvature condensation and twinning. (a) The axial location d_y (along the symmetry axis) of the condensate as a function of normalized indentation δ/R for different thicknesses (t/R as shown in the legend), with the dash-dotted lines showing saturation. The stars denote experimental data obtained from [7]. The dark-blue dashed line corresponds to the linear scaling law $d_y \sim \delta$ in the initial stages, before the onset of softening behavior. (b) The defect location d_x as a function of the indentation follows the simple law $d_x \sim (\delta - \delta_{bif})^{1/2}$ (dashed line) in the neighborhood of the bifurcation from one to two defects.

the curvature of the shell along the cylinder axis, and w is the average width of the parabolic crease. Stretching in the vicinity of the crease is primarily due to the nonvanishing Gauss curvature of the crease $\kappa_G \approx \frac{1}{R}\frac{\delta}{dw}$. Then, we may write the stretching energy $E_S \sim Et\gamma^2 dw$, where the stretching strain $\gamma \sim \sigma/Et \approx \kappa_G w^2$ in terms of the in-plane stress $\sigma \sim Et\nabla^{-2}\kappa_G$. This last relation follows from the compatibility relation for the stresses in the Donnell–Föppl–von Kármán equation which reads $\nabla^2\sigma \sim -\kappa_G$ [13]. Minimizing the total energy $E_B + E_S$ yields $w \sim \sqrt{tR}$, which agrees with our simulations over the range explored [Fig. 5(b)], similar to the scaling for the circular ridge obtained during the partial inversion of an elastic spherical cap [6]. For very thin shells, the curvature condensate bifurcates into two which move to a location $\pm d_x$ on either side of the axis of symmetry as the indentation increases beyond a threshold. Indeed, symmetry

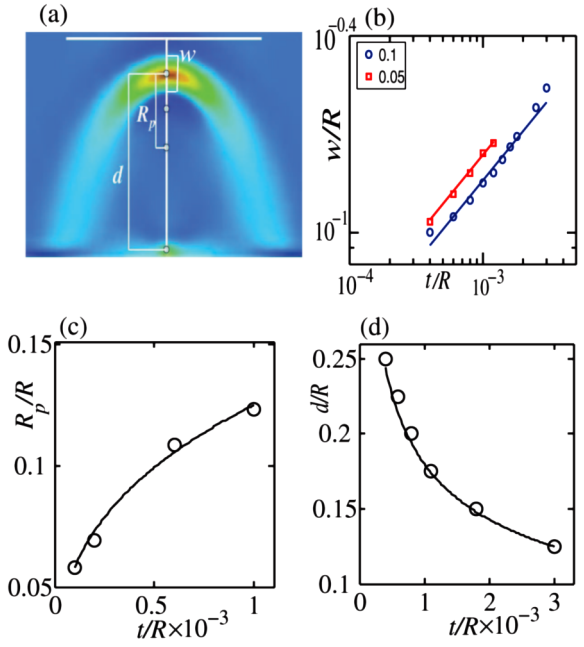

FIG. 5 (color online). Length scales characterizing the curvature condensate. (a) A magnified view of the curvature condensate in Fig. 2(f) showing the length scales w, R_p, and d. (b) The normalized width follows the scaling law $w/R \sim (t/R)^{1/2}$. (c) The normalized radius of curvature of the parabolic crease follows the scaling $R_p/R \sim (t/R)^{1/3}$. (d) The normalized location of the condensate follows the scaling law $d/R \sim (t/R)^{-1/3}$. In each case, the open symbols correspond to numerical simulations. There is no observed dependence of these scaling laws on the scaled indentation δ/R [for example, in Fig. 5(b), we show that the scaling of the width of the localized zone for two values of δ/R].

considerations thus demand that this supercritical pitchfork bifurcation must follow the scaling $d_x \sim (\delta - \delta_{\mathrm{bif}})^{1/2}$, consistent with what we observe in our numerical simulations [Fig. 4(b)].

Our studies are but a first step in understanding the question of defect formation and evolution in an elastic system. By indenting the edge of a semicylindrical shell we followed the exploration of the geometric localization of deformation experimentally and numerically. Although we can understand some aspects of the curvature condensate, much still remains to be done in trying to quantify this phenomenon which is fairly generic in curved shells. For example, our understanding of the condensation of curvature is qualitative—we do not know the conditions under which this would happen more generally. In addition, our description of twinning remains qualitative being based on symmetry arguments, not mechanistic ones. Our studies rely heavily on numerical simulations and experimental corroboration—much remains to be done in trying to quantify and supplement these notions using asymptotics and other semianalytical methods.

We thank B. Nyugen for help with some preliminary experiments, and M. Brenner, J. Hutchinson, and M. Weidman for useful discussions.

*Electronic address: lm@deas.harvard.edu

[1] D. R. Nelson, *Defects and Geometry in Condensed Matter Physics* (Cambridge University Press, Cambridge, England, 2002).
[2] A. E. Lobkovsky and T. A. Witten, Phys. Rev. E **55**, 1577 (1997).
[3] E. Cerda and L. Mahadevan, Phys. Rev. Lett. **80**, 2358 (1998); E. Cerda, S. Chaieb, F. Melo, and L. Mahadevan, Nature (London) **401**, 46 (1999).
[4] A. Boudaoud, P. Patrcio, Y. Couder, and M. Ben Amar, Nature (London) **407**, 718 (2000).
[5] E. Cerda and L. Mahadevan, Proc. R. Soc. A **461**, 671 (2005).
[6] For a recent accessible version, see A. Pogorelov, *Bending of Surfaces and Stability of Shells* (American Mathematical Society, Providence, 1988).
[7] J. M. F. G. Holst and C. R. Calladine, European Journal of Mechanics, A/Solids **13**, 3 (1994).
[8] D. Blair and A. Kudrolli, Phys. Rev. Lett. **94**, 166107 (2005).
[9] There is a dependence on the Poisson ratio, but this is weak and we will ignore it here.
[10] S. S. Antman, *Problems of Nonlinear Elasticity* (Springer, New York, 2003), 2nd ed.
[11] *Localization and Solitary Waves in Solid Mechanics*, edited by A. R. Champneys, G. W. Hunt, and J. M. T. Thompson, Advanced Series in Nonlinear Dynamics (World Scientific, Singapore, 1999).
[12] T. Liang and T. A. Witten, Phys. Rev. E **71**, 016612 (2005).
[13] E. H. Mansfield, *The Bending and Stretching of Plates* (Pergamon, New York, 1989), 2nd ed.